analytical chemistry

pubs.acs.org/ac Article

Capture of Electrochemically Generated Fleeting Carbazole Radical Cations and Elucidation of Carbazole Dimerization Mechanism by Mass Spectrometry

Chengyuan Liu, Qi Wang, Brian E. Hivick, Yongling Ai, Pier Alexandre Champagne, Yang Pan,* and Hao Chen*

Cite This: https://dx.doi.org/10.1021/acs.analchem.0c01223 Read Online

ACCESS | Metrics & More | Article Recommendations | Supporting Information

ABSTRACT: The capture of reactive intermediates is important for the elucidation of reaction mechanisms. We report the first observation of electrochemically generated, short-lived radical cations of carbazole ($t_{1/2} \approx 97\ \mu s$) and two N-substituted carbazole derivatives by mass spectrometry. In addition, online investigation of the reactivity of electrochemically generated carbazole radical cations supports that the carbazole dimerization mechanism involves the reaction of one radical cation with one neutral molecule rather than the previously proposed coupling of two radical cations.

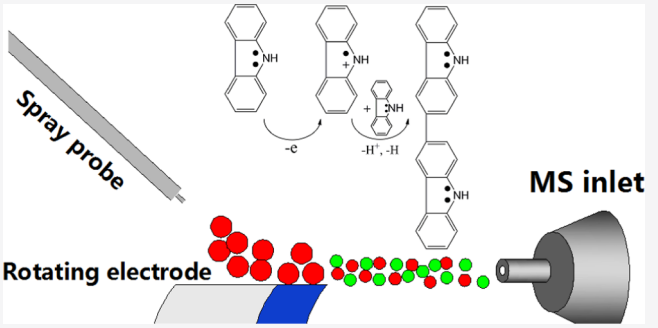

INTRODUCTION

The electrochemical oxidation of carbazole (CBZ) and its derivatives is a promising method to synthesize dimeric indole alkaloids[1] and prepare polycarbazoles,[2−5] which are very useful materials in making sensors[6] and photovoltaic devices.[7,8] Due to the planar geometry of the carbazole moiety, these electrochemically generated carbazole radical ions are unstable and react rapidly via dimerization reaction.[9−11]

The rate constants for the dimerization of CBZ, 9-(*p*-tolyl)CBZ (TCBZ), and 9-phenylcarbazole (PCBZ) have been determined to be in the range of 10^6 to 10^7 M^{-1} s^{-1}.[9,10,12] Because of this fast dimerization reaction, the life times of these carbazole radical cations are short (their half-life times are less than 1 ms at 1 mM concentration), and therefore, the detection of these species has been challenging. Previously, the CBZ radical cation ($CBZ^{+\bullet}$) generated from chemical oxidation was reported to be stabilized as $CBZ^{+\bullet}-BF4^-$,[13] but a later work indicated that the observed ion was probably the bicarbazyl radical cation.[14] Heinze et al. tried to detect the radical cations of both PCBZ and structurally similar compound triphenylamine (TPA), using *in situ* UV/vis spectrometry, but could only detect $TPA^{+\bullet}$.[15,16] The $PCBZ^{+\bullet}$ in acetonitrile (MeCN) was only observed by absorption spectroscopy by electron-transfer stopped-flow method.[17] The $CBZ^{+\bullet}$ was also detected based on a luminescence signal generated upon trapping reaction by a bis-[l,2,3-trimethyl-2,3-dihydrobenzimidazolyl-(2)]/luminophor system.[18] Moreover, the CBZ electro-oxidation has been extensively studied by cyclic voltammetry,[9] rotating disk voltammetry,[10] and electron spin resonance spectroscopy,[19] and the coupling of two radical cations was proposed to contribute to the dimer formation (Scheme 1, route A).[9,19] Compared to the techniques mentioned above which detect intermediates based on absorption spectroscopy, luminescence signals, voltammetric waves, and so forth, mass spectrometry (MS) is advantageous

Scheme 1. Proposed Oxidation and Dimerization Mechanism of CBZ, PCBZ, and TCBZ

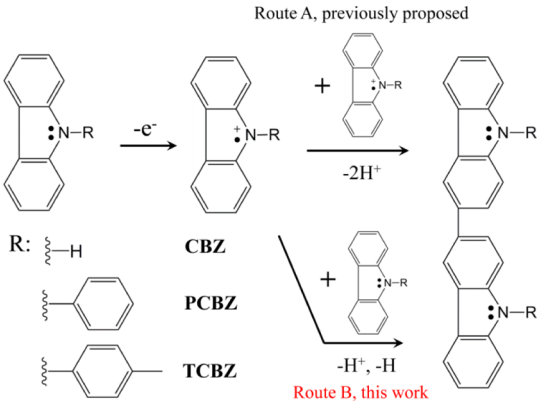

Received: March 20, 2020
Accepted: October 6, 2020

in detecting elusive reaction intermediates as the MS measurement has high specificity due to the capability of providing accurate mass information. Furthermore, structural information offered by tandem MS analysis improves the detection specificity. MS has been shown to be powerful for identifying electrochemical reaction intermediates.[20−34]

Herein, we propose the detection of these carbazole radical cation intermediates during electrochemical oxidation of CBZs by using desorption electrospray ionization MS (DESI−MS).[35−38] The combination of MS with electrochemistry (EC) has been one focus in our laboratory, which has been shown to have applications in protein structure analysis, quantitative proteomics, and reaction mechanism elucidation.[23,39−47] With the success of their detection by MS, we were able to further investigate the reactivity of carbazolium radical cations, and our data supported that the CBZ dimerization involves the reaction of one radical cation with one neutral molecule (Scheme 1, route B). Such a mechanistic elucidation would be fundamentally important in understanding the polymerization of CBZ materials.

EXPERIMENTAL SECTION

Chemicals. Ammonium acetate was obtained from Spectrum Chemical Mfg. Corp. (Gardena, CA, USA) with >97% purity. CBZ (95%) was purchased from Alfa Aesar (Karsruhe, Germany), and CBZ-d8 (98.7%) was bought from CDN Isotopes (Quebec, Canada). Tris(4-bromophenyl)-aminium hexachloroantimonate, 1-butyl-3-methylimidazolium chloride (98%), TCBZ (> 98%), and 3,3′-bicarbazyl (3,3′-BCBZ) were bought from TCI Corp. (Tokyo, Japan). PCBZ (97%) and *N*,*N*′-diphenyl-3,3′-bicarbazyl (>98%) were obtained from Sigma-Aldrich. All chemicals were used without further purification.

Apparatus. The experimental design shown in Figure 1 greatly resembles the waterwheel setup that was previously

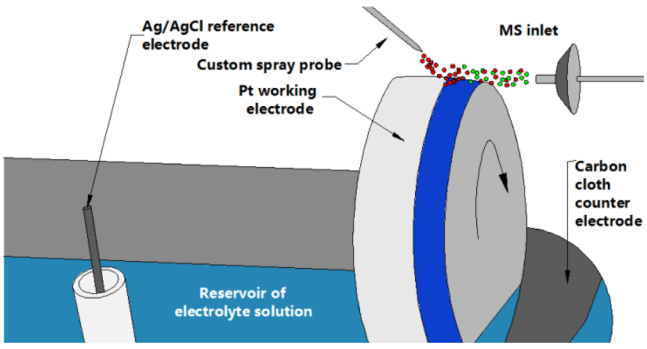

Figure 1. Experimental setup used for detection of electrochemical reaction intermediates of CBZs, employing a rotating waterwheel electrode. Wheel rotation is indicated by the curved arrow.

reported,[23,39,40] which employed a round rotating platinum working electrode immersed in 9:1 H_2O/MeCN solution containing 1 mM ammonium acetate as electrolyte. The platinum working electrode was fashioned from a Pt crucible and formed onto a Teflon disc. The counter electrode was a piece of plain carbon cloth fabric from AvCarb Material Solutions (Lowell, MA), and an Ag/AgCl reference electrode was purchased from BASi (West Lafayette, IN). The working electrode was rotated by a low voltage brush-type DC motor. The distance between the working electrode surface and the mass spectrometer inlet was ca. 2 mm. As the working electrode rotates, a thin layer of liquid film (ca. 1 mm thick) formed on the working electrode surface. The Ag/AgCl reference electrode and plain carbon cloth counter electrode were immersed in the reservoir of electrolyte solution. A metal contact (not shown) rested against the platinum working electrode surface to complete the three-electrode system. A CV-27 potentiostat (Bioanalytical Systems, West Lafayette, IN, USA) was used to apply a potential across the three electrodes. Above the rotating waterwheel electrode, a custom DESI spray probe (inner fused silica capillary: 100 μm ID and 150 μm OD and outer fused silica capillary: 250 μm ID and 350 μm OD) directed a spray of sample microdroplets to the working electrode surface, and the electrochemical reaction intermediates on the electrode surface were then transferred to a Q Exactive Plus mass spectrometer (Thermo Fisher Scientific, Indianapolis, IN, USA) for detection. Analyte solution was infused through the DESI emitter with the assistance of nebulizing N_2 gas (170 psi), and the emitter was positioned ∼2 mm above the electrode surface. In order to minimize in-source oxidation in DESI,[48,49] no high voltage was applied to the spray probe (therefore, the DESI spray emitter in this case was equivalent to a sonic spray source). For all experiments, the ion transfer capillary was held at 275 °C. The resolution was set to 140,000 at m/z = 200 for the CBZ experiments and 280,000 at m/z = 200 for the PCBZ and TCBZ experiments. Electrolysis experiments were set to run with zero potential applied to the working electrode for 30 s followed by application of an oxidation potential for 30 s. This was repeated three times to determine if the observation was reproducible within a single run.

For all the nanoelectrospray ionization (nanoESI) experiments, 2500−3000 V was applied and sample injection flow rate was set at 1−2 μL/min. For the online liquid sample DESI experiment, MeCN/H_2O/formic acid (v/v/v = 50:50:1) was infused through a DESI emitter at a flow rate of 20 μL/min and 3500 V was applied to assist the solvent spray.

In order to electrochemically generate the CBZ or CBZ-d_8 radical cation for the dimerization reaction, a μ-PrepCell (Antec BV, Zoeterwoude, The Netherlands) equipped with a glassy carbon working electrode (12 × 30 mm^2) was employed for electrochemical oxidation. A Roxy potentiostat (Antec BV, Zoeterwoude, Netherlands) was used to apply potential to the cell.

In order to quantify the dimer's concentration generated from 24 h chemical oxidation of CBZ, thermal desorption atmosphere pressure photoionization mass spectrometry (TD-APPI-MS) was used. The detail of this method had been described in detail elsewhere.[50] All data were analyzed using the Qual Browser feature of the Xcalibur program (Thermo Fisher Scientific).

RESULTS AND DISCUSSION

Capture of Short-Lived Radical Cations of CBZ, TCBZ, and PCBZ. As shown in Scheme 1, CBZ, TCBZ, and PCBZ are proposed to first generate radical cations by electrochemical oxidation,[2,9,10,19] which subsequently undergo dimerization. As reported by other groups, the 3- and 6-positions of the oxidized CBZ moiety have relatively high spin densities, and 3,3′-bicarbazyl is the main dimerization product in acidic solution.[2,9,51]

When 1 mM of CBZ in 1:1 MeCN/H_2O with 1% formic acid was sprayed at an injection flow rate of 50 μL/min onto

https://dx.doi.org/10.1021/acs.analchem.0c01223
Anal. Chem. XXXX, XXX, XXX−XXX

the working electrode rotating at 1 rev/s, the protonated CBZ was observed at *m/z* 168.0803 (Figure 2a, theoretical *m/z*

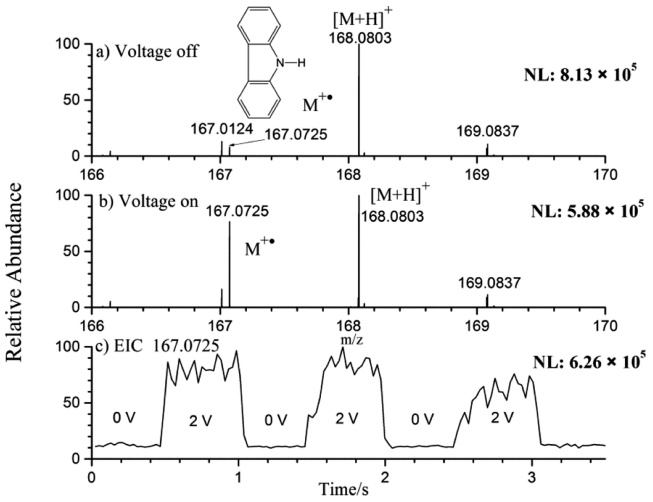

Figure 2. Positive-ion mode MS spectra of CBZ with (a) 0 and (b) 2 V applied to the rotating working electrode. (c) Extracted ion chromatogram for *m/z* 167.0725 as a function of the applied oxidation potential.

168.0808, error −3.0 ppm), and a small peak corresponding to $CBZ^{+\bullet}$ at *m/z* 167.0725 (Figure 2a, theoretical *m/z* 167.0730, error −3.0 ppm) was also detected. Formation of the $CBZ^{+\bullet}$ ion could be attributed to in-source oxidation from the spray ionization process[52] (oxidation of CBZ was observed during the ionization of standard CBZ by SSI, Figure S1, Supporting Information). When an oxidation potential of 2.0 V was applied onto the rotating working electrode, an almost 10-fold increase (from 6.4×10^4 to 4.5×10^5) of signal intensity at *m/z* 167.0725 (Figure 2b) was observed. Upon collision-induced dissociation (CID), fragments at *m/z* 166 and 140 were formed by losses of H and HCN neutrals from $CBZ^{+\bullet}$ at *m/z* 167.0725 (Figure S2a, Supporting Information), consistent with its structural assignment. The correlation of the ion intensity with the applied oxidation potential (Figure 2c) strongly suggests the formation of $CBZ^{+\bullet}$ via electrochemical oxidation of CBZ. When isotope-labeled CBZ-d_8 was used to replace CBZ in the experiment, the radical cation of CBZ-d_8 at *m/z* 175.1233 (theoretical *m/z* 175.1232, error 0.6 ppm) was also observed (Figure S3a−c, Supporting Information). Based on the average intensity change of the protonated CBZ upon electro-oxidation of three repetitive experiments, about 22% CBZ was consumed in the electrolysis, and the concentration of newly formed $CBZ^{+\bullet}$ was approximately 0.22 mM. According to the estimated coupling rate constant k (10^7 M^{-1} s^{-1}),[9] the half-life ($t_{1/2}$) of $CBZ^{+\bullet}$ is roughly 97 μs (Supporting Information) based on the radical cation/neutral reaction pathway proposed in this study (Route B, Scheme 1). A peak at *m/z* 332.1297 was also observed, attributed to the radical cation of 3,3′-bicarbazyl (3,3′-BCBZ) (theoretical *m/z* 332.1308, error −3.3 ppm, Figure S2b,c, Supporting Information). Upon CID, $3,3'\text{-BCBZ}^{+\bullet}$ gave rise to fragment ions of *m/z* 331, 330, and 306 by losses of H, 2H, and C_2H_2 neutrals (Figure S2d, Supporting Information), respectively, consistent with the CID spectrum of the $3,3'\text{-BCBZ}^{+\bullet}$ generated from nanoelectrospray ionization (nanoESI) of authentic 3,3′-BCBZ (Figure S2e, Supporting Information). The ion signal of $3,3'\text{-BCBZ}^{+\bullet}$ also correlated well with the applied oxidation potential (Figure S2f, Supporting Information), indicating that it stemmed from electrochemical oxidation of CBZ. It should be noted that the 9-position of $CBZ^{+\bullet}$ is not blocked, and thus, 9,9′-bicarbazyl could be formed via N−N coupling.[53] In order to examine whether or not 9,9′-bicarbazyl forms, 1 mM of CBZ-d_8 in 1:1 MeCN/H_2O with 1% formic acid was sprayed onto the working electrode. As shown in Figure S3d−f (Supporting Information), when the oxidation potential of 2.0 V was applied, only $3,3'\text{-BCBZ-d}_{14}{}^{+\bullet}$ at *m/z* 346.2185 (theoretical *m/z* 346.2187, error −0.6 ppm) was resulted, by loss of 2D from CBZ dimerization, suggesting that 9,9′-bicarbazyl (theoretical *m/z* 348.2312) was not formed. Indeed, the literature[9] reported a higher ionization potential of 9,9′-BCBZ (1.8 V) than of 3,3′-BCBZ (1.2 V). However, under the applied oxidation potential of 2 V used in our experiment, we would expect the generation and detection of the 9,9′-BCBZ radical cation, if 9,9′-BCBZ were present.

Two other N-substituted CBZs, TCBZ and PCBZ, were also examined by spraying 1 mM sample solution at an infusion rate of 20 μL/min onto the working electrode rotating at 1 rev/s. The dimerization rate constant for $TCBZ^{+\bullet}$ was estimated to be $8(\pm4)\times10^6$ M^{-1} s^{-1}.[10] The second-order rate constant for $PCBZ^{+\bullet}$ was $9(\pm6)\times10^7$ M^{-1} s^{-1} obtained by using rotating disk voltammetry[10] and later the dimerization process was shown to follow second-order kinetics with a rate constant of 1.2×10^6 M^{-1} s^{-1} by cyclic voltammetry.[12] At 1 mM concentration, both $TCBZ^{+\bullet}$ and $PCBZ^{+\bullet}$ are short-lived, and their half-lives should be less than 1 ms. Before the oxidation potential was applied to the cell (Figure 3a), the protonated

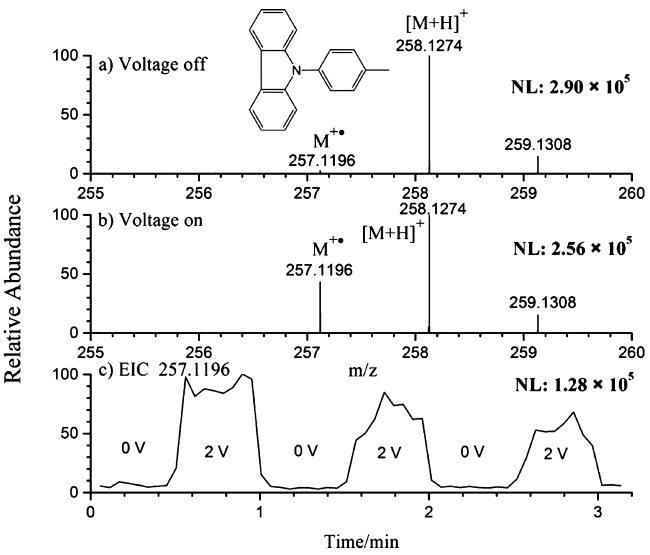

Figure 3. Positive-ion mode MS spectra of TCBZ with (a) 0 and (b) 2 V applied to the rotating working electrode. (c) EIC for *m/z* 257.1196 as a function of the applied oxidation potential.

TCBZ at *m/z* 258.1274 was observed, along with a small peak of the $TCBZ^{+\bullet}$ at *m/z* 257.1196 (likely due to in-source oxidation). When the cell was turned on, $TCBZ^{+\bullet}$ at *m/z* 257.1196 (theoretical *m/z* 257.1199, error −1.1 ppm) was clearly seen (Figure 3b), and its signal intensity exhibited a clear response to the applied potential (Figure 3c). Upon CID, this ion yielded a fragment at *m/z* 242 from loss of CH_3 (Figure S4a, Supporting Information). In addition, the formation of the *N*,*N*′-ditolyl-3,3′-bicarbazyl radical cation at *m/z* 512.2241 (theoretical *m/z* 512.2247, error −1.2 ppm,

https://dx.doi.org/10.1021/acs.analchem.0c01223
Anal. Chem. XXXX, XXX, XXX−XXX

Figure S4b,c, Supporting Information) occurred. Upon CID, m/z 512 dissociates into m/z 421 by loss of a toluene molecule C_7H_8 (Figure S4d, Supporting Information). Similar results were obtained for PCBZ. $PCBZ^{+\bullet}$ at m/z 243.1040 (theoretical m/z 243.1043, error −1.2 ppm, Figure S5a−c, Supporting Information) was observed as a result of electrochemical oxidation of PCBZ. Upon CID of the ion at m/z 243.1040 (Figure S5d, Supporting Information), a major product at m/z 217 by loss of C_2H_2 neutral was detected. The dimer radical cation was detected at m/z 484.1926 (theoretical m/z 484.1934, error −1.6 ppm, Figure S5e−i, Supporting Information). These results above clearly show that transient radical cations of various CBZs could be detected by MS directly.

Elucidation of the CBZ Dimerization Mechanism. With the success in the detection of radical cations of CBZs, we proceeded to further investigate the mechanism of CBZ dimerization reaction, a key step in the process of converting CBZs into useful materials. As mentioned above, the proposed mechanism involves the reaction of one carbazole radical cation and another carbazole radical cation (Scheme 1, route A). For the dimerization process, due to structural similarities, carbazole radical cations were always assumed to be dimerized via the same process as aromatic amine radical cations, which were dimerized via a radical cation-radical cation coupling mechanism.[54−56] However, the proposed mechanism lacks experimental evidence. In theory, as the radical cation is very unstable, it could couple with either another radical cation or with a parent neutral molecule, forming the more stable dicarbazyl.[2] The latter pathway appears to be more energetically favored as the former process involves the unfavorable charge−charge repulsion between two radical cations. Indeed, one later report indicated that neutral PCBZ can accelerate the dimerization of $PCBZ^{+\bullet}$.[17] Nonetheless, no study in this regard was conducted. We reason that MS could be used to elucidate the true reaction mechanism as we could capture and detect radical cations of CBZ and its derivatives, as shown above.

In our approach, we designed a simple apparatus (Figure 4a) to allow CBZ to be electrochemically oxidized into $CBZ^{+\bullet}$, followed with fast mixing with isotope-labeled CBZ-d_8. The formation of a heterogeneous dimer between $CBZ^{+\bullet}$ and CBZ-d_8 would provide evidence for the occurrence of the reaction between one carbazolium radical cation and one neutral CBZ molecule. The use of CBZ-d_8 in this experiment is for the differentiation purpose as the dimer of CBZ will form upon the CBZ electro-oxidation process. As shown in Figure 4a, the apparatus consisted of a thin-layer electrochemical flow cell equipped with glass carbon working electrode (30 × 12 mm^2, ANTEC BV, the Netherlands) that was connected with a Tee mixer using a short piece of capillary (100 μm ID, 198 μm OD, 2.5 cm long), which was used in our work for confirming chain reaction mechanism in photoredox catalytic reactions.[57] A solution of 0.5 mM CBZ in 100 μM lithium triflate (LiOTf, serving as an electrolyte) in MeCN was infused through the electrochemical flow cell via channel 1 to generate $CBZ^{+\bullet}$ by electrochemical oxidation. The generated $CBZ^{+\bullet}$ was detected using liquid sample DESI−MS[41] (Figure S6, Supporting Information). The injection flow rate for CBZ solution was 70 μL/min, and the high flow rate was used to facilitate the transfer of the $CBZ^{+\bullet}$ for reaction. In the channel 2 of the Tee mixer, either pure solvent MeCN or 0.5 mM CBZ-d_8 in MeCN was infused to mix with the $CBZ^{+\bullet}$-containing solution coming from the cell. The solution flowing out of the Tee mixer was

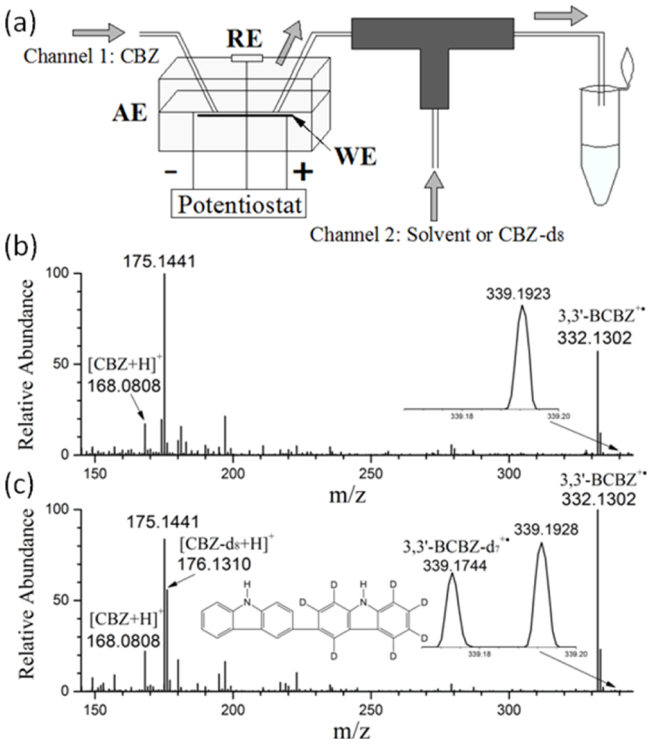

Figure 4. (a) Schematic showing the experimental setup for investigating the reaction between the CBZ radical cation and neutral CBZ-d_8. AE, RE, and WE represent auxiliary electrode, reference electrode, and working electrode, respectively. NanoESI-MS spectra of the collected reaction mixture when solvent (b) or CBZ-d_8 (c) was flowed through channel 2.

collected and analyzed by nanoESI−MS. As shown in Figure 4b, when MeCN was introduced, the heterogeneous dimer 3,3′-BCBZ-d_7 (structure shown in Figure 4c) was not observed. However, when the MeCN was replaced by CBZ-d_8, the peak at m/z 339.1744 corresponding to the 3,3′-BCBZ-d_7 radical cation (theoretical m/z 339.1747, error −0.9 ppm) appeared (Figure 4c). Note that m/z 339.1744 was not an artifact of the nanoESI ionization process, as the heterogeneous dimer 3,3′-BCBZ-d_7 radical cation was not observed in a control experiment when 0.25 mM CBZ and 0.25 mM CBZ-d_8 in MeCN containing 50 μM LiOTf was directly ionized by nanoESI (Figure S7a, Supporting Information). The reason for the observation of the 3,3′-BCBZ-$d_7^{+\bullet}$ ion rather than the protonated 3,3′-BCBZ-d_7 was likely due to the in-source oxidation of nanoESI. Indeed, when 3,3′-BCBZ dissolved in 50 μM LiTOf solution was ionized directly, oxidation was observed (Figure S7b, Supporting Information). For the T-junction experiment, the MS^2 mass spectra of the ion at m/z 339.1744 in Figure 4c are shown in Figure S8. Upon CID, 3,3′-BCBZ-$d_7^{+\bullet}$ at m/z 339.1744 showed similar fragments as 3,3′-BCBZ at m/z 332.1296 (Figure S2d, Supporting Information) and gave rise to fragment ions of m/z 338, 337, 336, and 311 by losses of H, D, HD, and C_2D_2 neutrals, respectively, consistent with the assigned structures. These results directly support that the CBZ radical cation does react with a neutral CBZ molecule to form dimer. Note that, in consideration of the short life time of the CBZ radical cation, it would be surprising that the CBZ radical cation generated from the electrochemical cell could reach the Tee junction to react with CBZ-d_8. By estimation (see calculation in Supporting

https://dx.doi.org/10.1021/acs.analchem.0c01223
Anal. Chem. XXXX, XXX, XXX−XXX

Information), it turns out that, although the concentration of the CBZ radical cation would decrease significantly (Supporting Information), a small fraction of the CBZ radical cation could survive and be detected by liquid sample DESI experiment (Figure S6, Supporting Information). Also, this observation was in agreement with the weak intensity of m/z 339.1744, in comparison with m/z 332.1302.

In a similar experiment (Figure S9, Supporting Information), CBZ-d_8 was introduced via channel 1 for electrochemical oxidation to generate CBZ-d_8 radical cations, and CBZ was flowed through channel 2 for reaction via the Tee. NanoESI−MS spectra (background subtracted) of the collected reaction mixture again shows the presence of the 3,3′-BCBZ-d_7 radical cation of m/z 339.1750 (theoretical m/z 339.1747, error 0.9 ppm; Figure S9b, Supporting Information), suggesting that the radical cation/neutral reaction takes place.

In addition, chemical oxidation of CBZ to form radical cations followed by mixing with CBZ-d_8 was also attempted. The result was in good agreement with the result from the electrochemical oxidation experiment shown above. In the experiment, the samples were prepared according to the workflow depicted in Figure S10a (Supporting Information). First, 100 μL of 1 mM CBZ in MeCN was oxidized directly by an excess amount of tris(4-bromophenyl)aminium hexachloroantimonate, a well-known one-electron transfer oxidant (100 μL of 10 mM in MeCN). The resulting solution (Figure S11shows the partial oxidation of CBZ and the formation of a CBZ radical cation upon mixing the CBZ with the oxidant) was mixed with 100 μL of 1 mM CBZ-d_8 in MeCN. Again, nanoESI-MS analysis of the final reaction solution revealed the presence of the formation of heterogeneous dimer 3,3′-BCBZ-d_7 (measured m/z 339.1744, theoretical m/z 339.1747, error −0.9 ppm, Fig S10c, Supporting Information). Interestingly, when the CBZ-d_8 was also oxidized by the oxidant (for the generation of CBZ-$d_8^{+\bullet}$) prior to the mixing with the oxidized CBZ, the relative intensity of the 3,3′-BCBZ-d_7 peak (relative to the peak of butyl-3-methylimidazolium ion at m/z 139 from an added internal standard butyl-3-methylimidazolium chloride) became smaller (0.10 ± 0.03, in triplicate measurements, Figure S10b, Supporting Information), in comparison to that of the 3,3′-BCBZ-d_7 peak (0.54 ± 0.11) when CBZ-d_8 was not oxidized (Figure S10c, Supporting Information). This result does not support the formation of dimer via the radical cation-radical cation reaction pathway (Scheme 1, Route A). The reason for a lower yield 3,3′-BCBZ-d_7 (shown in Figure S10b) is likely that pre-oxidation of CBZ-d_8 reduced the amount of CBZ-d_8 neutral that was available for reacting with CBZ radical cations. Again, this result is in line with our hypothesis that the CBZ dimerization involves the reaction between the CBZ radical cation and one neutral CBZ molecule (Scheme 1, route B).

Further evidence was obtained using a partial chemical oxidation experiment. In this experiment, 500 μL of 0.5 mM oxidant (tris(4-bromophenyl)aminium hexachloroantimonate) was mixed with 500 μL of 10 mM CBZ in MeCN (CBZ is in excess amount). After mixing, the concentrations of oxidant and CBZ were 0.25 and 5 mM, respectively. After the mixture was shaken for 24 h to enable the oxidant to be completely consumed, the mixture was diluted 5 fold, and 6 μM nicotine was added as an internal standard for analysis by TD-APPI-MS.[57] If the 3,3′-BCBZ were formed via radical cation/neutral pathway, 0.25 mM dimer would be expected, as 0.25 mM oxidant in the reaction mixture would produce 0.25 mM CBZ radical cations which reacted with CBZ neutrals to form 0.25 mM 3,3′-BCBZ. On the other hand, if CBZ were dimerized via radical cation/radical cation pathway, the dimer concentration would be halved and become 0.125 mM, as two CBZ radical cations would form one molecule of dimer. In this experiment, TD-APPI-MS was used for the dimer product quantification due to its higher ionization sensitivity for 3,3′-BCBZ and the reduced ion suppression effect compared with nanoESI (Figure S12, Supporting Information). Based on the linear relationship in Figure S12d, the concentration of 3,3′-BCBZ in the 24 h chemical oxidation of CBZ was calculated to be 0.24 mM, which is close to 0.25 mM, as predicted by the radical cation/neutral reaction mechanism.

CONCLUSIONS

In summary, transient radical cations of CBZ, PCBZ, and TCBZ generated from electrochemical oxidation events were successfully captured and detected online by DESI−MS. The one-electron redox reaction was demonstrated to be the first step in this process. The power of DESI−MS in identifying short-lived electrochemical intermediates was demonstrated. In addition, radical cation-neutral substrate coupling mechanism was demonstrated to be responsible for CBZ dimerization based on our experimental results from online reactivity test for electrochemically generated CBZ radical cations and quantitative analysis of the dimer amount from chemical oxidation of CBZ. Nevertheless, the possibility of radical cations/radical cations could not be completely excluded, for which further study is in need.

ASSOCIATED CONTENT

Supporting Information

The Supporting Information is available free of charge at https://pubs.acs.org/doi/10.1021/acs.analchem.0c01223.

Additional MS data and radical cation half-life time calculations (PDF)

AUTHOR INFORMATION

Corresponding Authors

Yang Pan − *National Synchrotron Radiation Laboratory, University of Science and Technology of China, Hefei 230029, China;* orcid.org/0000-0002-9360-3809; Email: panyang@ustc.edu.cn

Hao Chen − *Department of Chemistry & Environmental Science, New Jersey Institute of Technology, Newark, New Jersey 07102, United States; Department of Chemistry & Biochemistry, Ohio University, Athens, Ohio 45701, United States;* orcid.org/0000-0001-8090-8593; Email: hao.chen.2@njit.edu

Authors

Chengyuan Liu − *Department of Chemistry & Environmental Science, New Jersey Institute of Technology, Newark, New Jersey 07102, United States; National Synchrotron Radiation Laboratory, University of Science and Technology of China, Hefei 230029, China*

Qi Wang − *Department of Chemistry & Environmental Science, New Jersey Institute of Technology, Newark, New Jersey 07102, United States*

Brian E. Hivick − *Department of Chemistry & Biochemistry, Ohio University, Athens, Ohio 45701, United States*

https://dx.doi.org/10.1021/acs.analchem.0c01223
Anal. Chem. XXXX, XXX, XXX−XXX

Yongling Ai − *Department of Chemistry & Environmental Science, New Jersey Institute of Technology, Newark, New Jersey 07102, United States*

Pier Alexandre Champagne − *Department of Chemistry & Environmental Science, New Jersey Institute of Technology, Newark, New Jersey 07102, United States;* orcid.org/0000-0002-0546-7537

Complete contact information is available at: https://pubs.acs.org/10.1021/acs.analchem.0c01223

Notes

The authors declare no competing financial interest.

■ ACKNOWLEDGMENTS

The financial support from NSF (CHE-1915878 and CHE-1428787) is gratefully acknowledged.

■ REFERENCES

(1) Rosen, B. R.; Werner, E. W.; O'Brien, A. G.; Baran, P. S. *J. Am. Chem. Soc.* **2014**, *136*, 5571−5574.
(2) Karon, K.; Lapkowski, M. *J. Solid State Electrochem.* **2015**, *19*, 2601−2610.
(3) Ates, M.; Uludag, N. *J. Solid State Electrochem.* **2016**, *20*, 2599−2612.
(4) Macit, H.; Sen, S.; Saçak, M. *J. Appl. Polym. Sci.* **2005**, *96*, 894−898.
(5) Fulghum, T.; Karim, S. M. A.; Baba, A.; Taranekar, P.; Nakai, T.; Masuda, T.; Advincula, R. C. *Macromolecules* **2006**, *39*, 1467−1473.
(6) Nie, H.; Sun, G.; Zhang, M.; Baumgarten, M.; Müllen, K. *J. Mater. Chem.* **2012**, *22*, 2129−2132.
(7) Hu, L.; Cai, W.; Zhao, W.; Zhang, B.; Yang, W. *J. Macromol. Sci., Part A: Pure Appl.Chem.* **2015**, *52*, 155−161.
(8) Brunner, K.; van Dijken, A.; Börner, H.; Bastiaansen, J. J. A. M.; Kiggen, N. M. M.; Langeveld, B. M. W. *J. Am. Chem. Soc.* **2004**, *126*, 6035−6042.
(9) Ambrose, J. F.; Nelson, R. F. *J. Electrochem. Soc.* **1968**, *115*, 1159−1164.
(10) Ambrose, J. F.; Carpenter, L. L.; Nelson, R. F. *J. Electrochem. Soc.* **1975**, *122*, 876−894.
(11) Morkovnik, A. S.; Okhlobystin, O. Y. *Chem. Heterocycl. Compd.* **1980**, *16*, 777−794.
(12) Heinze, J.; Hinkelmann, K.; Dietrich, M.; Mortensen, J. *Ber. Bunsenges. Phys. Chem.* **1985**, *89*, 1225−1229.
(13) Ledwith, A.; Sambhi, M. *Chem. Commun.* **1965**, *4*, 64−65.
(14) Iles, D. H.; Ledwith, A. *Chem. Commun.* **1968**, *9*, 498−499.
(15) Marcoux, L. S.; Adams, R. N.; Feldberg, S. W. *J. Phys. Chem.* **1969**, *73*, 2611−2614.
(16) Yurchenko, O.; Freytag, D.; zur Borg, L.; Zentel, R.; Heinze, J.; Ludwigs, S. *J. Phys. Chem. B* **2012**, *116*, 30−39.
(17) Oyama, M.; Matsui, J. *Bull. Chem. Soc. Jpn* **2004**, *77*, 953−957.
(18) Pragst, F.; Niazymbetov, M. *J. Electroanal. Chem.* **1986**, *197*, 245−264.
(19) Fujita, H.; Yamauchi, J.; Ohyma-nishiguchi, H. *Nippon Kagaku Kaishi* **1989**, 1344−1350.
(20) Liu, Y.-M.; Perry, R. H. *J. Am. Soc. Mass Spectrom.* **2015**, *26*, 1702−1712.
(21) Liu, Y.-M.; Nicolau, B. G.; Gewirth, A. A. *Anal. Chem.* **2016**, *88*, 7171−7177.
(22) Qiu, R.; Zhang, X.; Luo, H.; Shao, Y. *Chem. Sci.* **2016**, *7*, 6684−6688.
(23) Brown, T. A.; Chen, H.; Zare, R. N. *J. Am. Chem. Soc.* **2015**, *137*, 7274−7277.
(24) Cheng, H.; Yan, X.; Zare, R. N. *Anal. Chem.* **2017**, *89*, 3191−3198.
(25) Yu, J.; Zhou, Y.; Hua, X.; Liu, S.; Zhu, Z.; Yu, X.-Y. *Chem. Commun.* **2016**, *52*, 10952−10955.
(26) Lu, J.; Hua, X.; Long, Y.-T. *Analyst* **2017**, *142*, 691−699.
(27) van den Brink, F. T. G.; Büter, L.; Odijk, M.; Olthuis, W.; Karst, U.; van den Berg, A. *Anal. Chem.* **2015**, *87*, 1527−1535.
(28) Diehl, G.; Karst, U. *Anal. Bioanal. Chem.* **2002**, *373*, 390−398.
(29) Gun, J.; Bharathi, S.; Gutkin, V.; Rizkov, D.; Voloshenko, A.; Shelkov, R.; Sladkevich, S.; Kyi, N.; Rona, M.; Wolanov, Y.; Rizkov, D.; Koch, M.; Mizrahi, S.; Pridkhochenko, P. V.; Modestov, A.; Lev, O. *Isr. J. Chem.* **2010**, *50*, 360−373.
(30) Permentier, H.; Bruins, A.; Bischoff, R. *Mini Rev. Med. Chem.* **2008**, *8*, 46−56.
(31) Zhou, F.; Van Berkel, G. J. *Anal. Chem.* **1995**, *67*, 3643−3649.
(32) Wang, Z.; Zhang, Y.; Liu, B.; Wu, K.; Thevuthasan, S.; Baer, D. R.; Zhu, Z.; Yu, X.-Y.; Wang, F. *Anal. Chem.* **2017**, *89*, 960−965.
(33) Clark, E. L.; Bell, A. T. *J. Am. Chem. Soc.* **2018**, *140*, 7012−7020.
(34) Khanipour, P.; Löffler, M.; Reichert, A. M.; Haase, F. T.; Mayrhofer, K. J. J.; Katsounaros, I. *Angew. Chem., Int. Ed.* **2019**, *131*, 7351−7355.
(35) Miao, Z.; Chen, H. *J. Am. Soc. Mass Spectrom.* **2009**, *20*, 10−19.
(36) Miao, Z.; Wu, S.; Chen, H. *J. Am. Soc. Mass Spectrom.* **2010**, *21*, 1730−1736.
(37) Takats, Z.; Wiseman, J. M.; Gologan, B.; Cooks, R. G. *Science* **2004**, *306*, 471−473.
(38) Venter, A. R.; Douglass, K. A.; Shelley, J. T.; Hasman, G., Jr; Honarvar, E. *Anal. Chem.* **2014**, *86*, 233−249.
(39) Brown, T. A.; Chen, H.; Zare, R. N. *Angew. Chem., Int. Ed.* **2015**, *127*, 11335−11337.
(40) Brown, T. A.; Hosseini-Nassab, N.; Chen, H.; Zare, R. N. *Chem. Sci.* **2016**, *7*, 329−332.
(41) Li, J.; Dewald, H. D.; Chen, H. *Anal. Chem.* **2009**, *81*, 9716−9722.
(42) Zhang, Y.; Cui, W.; Zhang, H.; Dewald, H. D.; Chen, H. *Anal. Chem.* **2012**, *84*, 3838−3842.
(43) Zhang, Y.; Dewald, H. D.; Chen, H. *J. Proteome Res.* **2011**, *10*, 1293−1304.
(44) Xu, C.; Zheng, Q.; Zhao, P.; Paterson, J.; Chen, H. *J. Am. Soc. Mass Spectrom.* **2019**, *30*, 685−693.
(45) Ye, X.; Zhao, P.; Zhang, S.; Zhang, Y.; Wang, Q.; Shan, C.; Wojtas, L.; Guo, H.; Chen, H.; Shi, X. *Angew. Chem., Int. Ed.* **2019**, *58*, 17226−17230.
(46) Zhao, P.; Guo, Y.; Dewald, H. D.; Chen, H. *Int. J. Mass Spectrom.* **2019**, *443*, 41−45.
(47) Zhao, P.; Zare, R. N.; Chen, H. *J. Am. Soc. Mass Spectrom.* **2019**, *30*, 2398−2407.
(48) Benassi, M.; Wu, C.; Nefliu, M.; Ifa, D. R.; Volný, M.; Cooks, R. G. *Int. J. Mass Spectrom.* **2009**, *280*, 235−240.
(49) Pasilis, S. P.; Kertesz, V.; Van Berkel, G. J. *Anal. Chem.* **2008**, *80*, 1208−1214.
(50) Zhao, W.; Liu, C.; Yin, H.; Qi, K.; Xu, M.; Yang, J.; Pan, Y. *Anal. Methods* **2019**, *11*, 1304−1311.
(51) Maitland, P.; Tucker, S. H. *J. Chem. Soc.* **1927**, 1388−1392.
(52) Zivolic, F.; Zancanaro, F.; Favretto, D.; Ferrara, S. D.; Seraglia, R.; Traldi, P. *J. Mass Spectrom.* **2010**, *45*, 411−20.
(53) Desbene-Monvernay, A.; Lacaze, P.-C.; Dubois, J.-E. *J. Electroanal. Chem. Interfacial Electrochem.* **1981**, *129*, 229−241.
(54) Oyama, M.; Higuchi, T.; Okazaki, S. *J. Chem. Soc., Perkin Trans. 2* **2001**, 1287−1293.
(55) Yang, H.; Bard, A. J. *J. Electroanal. Chem.* **1991**, *306*, 87−109.
(56) Larumbe, D.; Gallardo, I.; Andrieux, C. P. *J. Electroanal. Chem.* **1991**, *304*, 241−247.
(57) Cai, Y.; Wang, J.; Zhang, Y.; Li, Z.; Hu, D.; Zheng, N.; Chen, H. *J. Am. Chem. Soc.* **2017**, *139*, 12259−12266.